New measurements of the coherent and incoherent neutron scattering lengths of $^{13}C$



2008 J. Phys.: Condens. Matter 20 045221

(http://iopscience.iop.org/0953-8984/20/4/045221)

J. Phys.: Condens. Matter **20** (2008) 045221 (14pp) doi:10.1088/0953-8984/20/04/045221

# New measurements of the coherent and incoherent neutron scattering lengths of $^{13}$C

**H E Fischer[1], J Neuefeind[2], J M Simonson[3], R Loidl[1,4] and H Rauch[4]**

[1] Institut Laue-Langevin, 6 rue Jules Horowitz, BP 156, 38042 Grenoble cedex 9, France
[2] Spallation Neutron Source, Oak Ridge National Laboratory, PO Box 2008 MS 6474, Oak Ridge, TN 37831, USA
[3] Center for Nanophase Materials Sciences, Oak Ridge National Laboratory, PO Box 2008 MS 6493, Oak Ridge, TN 37831, USA
[4] E141 Atominstitut der Österreichischen Universitäten, Stadionallee 2, 1020 Wien, Österreich, Austria

E-mail: fischer@ill.fr

Received 11 September 2007, in final form 6 December 2007
Published 8 January 2008
Online at stacks.iop.org/JPhysCM/20/045221

**Abstract**

The techniques of neutron interferometry and neutron diffraction were used to determine the coherent and incoherent neutron scattering lengths of $^{13}$C. From a neutron interferometry measurement of the optical path difference in liquid samples, $^{13}CS_2$ versus $^{nat}CS_2$, we obtain a bound coherent scattering length of $b_{coh,13C} = 6.542 \pm 0.003$ fm, which differs appreciably from the standard tabulated value of $6.19 \pm 0.09$ fm. The resulting contrast of only 0.106(3) fm with respect to $b_{coh,natC} = 6.6484 \pm 0.0013$ fm has consequences for neutron diffraction experiments involving $^{13}$C isotopic substitution. Combining our result for $b_{coh,13C}$ with precise neutron diffraction measurements of the self-scattering intensities of liquid samples, $^{13}CS_2$ versus $^{nat}CS_2$, and $^{13}CO_2$ versus $^{12}CO_2$, we deduce a bound incoherent scattering length of $b_{incoh,13C} = -0.42 \pm 0.24$ fm that is consistent with the standard tabulated value of $-0.52 \pm 0.09$ fm. The results presented here have required accurate measurements of small effects, for which particular attention has been given to the data analysis.

## 1. Introduction

Neutron scattering studies of condensed matter clearly require accurate values for the coherent $b_{coh}$ and incoherent $b_{incoh}$ scattering lengths of the elements present in the sample under study. In particular, isotopic substitution techniques in neutron diffraction, wherein chemically identical samples are prepared having different isotopic compositions, rely on accurate knowledge of the coherent scattering length contrast $\Delta b_{coh}$ between isotopes of a given element. In the case when $\Delta b_{coh}$ is rather small ($\lesssim$0.5 fm), inaccuracies in the $b_{coh}$ can lead to large relative errors.

Due to its omnipresence in organic, biological and macromolecular systems, the element carbon (C) is particularly attractive for isotopic substitution studies. Naturally occurring carbon ($^{nat}$C) has only two stable isotopes: $^{12}$C (98.89%) and $^{13}$C (1.11%). Experimental values for $b_{coh}$ and $b_{incoh}$ of natural carbon and its two isotopes are listed in standard references on neutron scattering lengths (Rauch and Waschkowski 2002, Sears 1992, Koester *et al* 1991, Mughabghab *et al* 1981).

The coherent neutron scattering length of $^{nat}$C was determined very accurately using the methods of gravity refraction (Koester and Nistier 1975) and neutron interferometry (Freund *et al* 1985) to be $b_{coh,natC} = 6.6484(13)$ fm.

For the $^{13}$C isotope, the currently accepted standard value of $b_{coh,13C} = 6.19(9)$ fm stems from a Christiansen filter experiment (Koester *et al* 1979) based on contrast-matching the small-angle scattering signal of a $K_2CO_3$ powder containing 90% $^{13}$C and 10% $^{12}$C, and agrees with an earlier result of 6.0(4) fm deduced from the scattering intensity of a $Ba^{13}CO_3$ powder (Koehler and Wollan 1952).

The high abundance of the $^{12}$C isotope allows a relatively precise coherent scattering length to be deduced from the currently accepted values for $^{13}$C and $^{nat}$C, rather than

 

through independent measurement, resulting in $b_{\mathrm{coh,12C}} = 6.6535(14)$ fm as tabulated by Rauch and Waschkowski (2002).

These standard tabulated values would therefore imply a coherent scattering length contrast of 0.46(9) fm between $^{13}$C and $^{\mathrm{nat}}$C, which is sufficient for isotopic substitution experiments using modern instrumentation on high-flux neutron sources. The technique of neutron diffraction with isotopic substitution (NDIS) is widely used to determine partial structure factors (PSFs) of structurally disordered systems such as liquids and glasses (see e.g. Fischer *et al* 2006 for a review). A sample's measured diffraction intensity is a weighted sum of PSFs each involving a pair of atomic species. The decomposition into individual PSFs requires the ability to vary the coherent scattering lengths in the sample, whence isotopic substitution. The Fourier transform of a PSF gives the corresponding partial pair-distribution function in real space, which expresses the probability of finding an atom of type A (e.g. carbon) at a certain distance from an atom of type B (e.g. oxygen). Partial pair-distribution functions derived from NDIS studies are an important source of information for understanding the structure of disordered systems.

There have been reports of $^{13}$C/$^{\mathrm{nat}}$C NDIS experiments by Turner *et al* (1991) for pure methanol and Kameda *et al* (2004) for sodium acetate solution. Turner *et al* (1991) report atomic coordination numbers that are too low by a factor of more than two, indicating that the scattering length contrast is smaller than the 0.46(9) fm expected from tabulated values. Furthermore, using single-crystal neutron diffraction methods, Young *et al* (1997) refined the crystal structure of a partially $^{13}$C-substituted organic molecule and found a very small scattering length contrast. In fact they refined an average $^{13}$C scattering length of 6.56(3) fm, a value that is completely consistent with our result of $b_{\mathrm{coh,13C}} = 6.542(3)$ fm. Finally, a recently attempted NDIS study on $CS_2$ (Mason 2005) also implies a smaller scattering length contrast than expected.

As concerns carbon's incoherent neutron scattering lengths, the spinless isotope $^{12}$C produces no incoherent neutron scattering, so that the incoherent scattering of $^{\mathrm{nat}}$C comes entirely from the presence of the rarely occurring $^{13}$C isotope. In the aforementioned study that obtained $b_{\mathrm{coh,13C}} = 6.19(9)$ fm, Koester *et al* (1979) also deduces a value of $b_{\mathrm{incoh,13C}} = \pm(2.3 + 0.8/-1.2)$ fm from the total scattering cross-section of $^{\mathrm{nat}}$C (Houk 1971) combined with his result for $b_{\mathrm{coh,13C}}$. However, due to the small abundance of $^{13}$C in natural carbon, his value for $b_{\mathrm{incoh,13C}}$ has very limited precision. The standard tabulated value of $b_{\mathrm{incoh,13C}} = -0.52(9)$ fm results from a polarized neutron scattering experiment that measured the nuclear polarization of $^{13}$C present in a sample of $Ba^{13}CO_3$ powder (Glättli *et al* 1979). This standard value for $b_{\mathrm{incoh,13C}}$ is marginally consistent with the theoretical value of $-0.4$ fm by Normand (1977), but the recent work of Aleksejevs *et al* (1998) suggests the smaller-magnitude value of $-0.26$ fm.

In view of the inconsistency among experimental results, and the importance of accurate values for the neutron scattering lengths of $^{13}$C in isotopic substitution studies, we decided to undertake neutron interferometry and neutron diffraction experiments to measure $b_{\mathrm{coh,13C}}$ and $b_{\mathrm{incoh,13C}}$. The choice of the liquid state for our $CS_2$ and $CO_2$ samples was motivated by two advantages: (1) a liquid sample can have a well defined and reproducible volume and geometry, which is capital for proper data normalization; (2) a liquid's diffraction pattern is a smoothly varying function that is easily fit and does not require detailed information about instrumental resolution. The simple linear intramolecular structure of $CS_2$ and $CO_2$ is also amenable to molecular dynamics (MD) simulations, which aided the analysis of our diffraction data. In addition, the symmetrical position of carbon in these molecules helps to reduce possible quantum effects arising from the isotopic mass difference (e.g. (Tomberli *et al* 2000, Badyal *et al* 2002)).

Our neutron interferometry experiment on liquid $^{13}CS_2$ and $^{\mathrm{nat}}CS_2$ resulted in $b_{\mathrm{coh,13C}} = 6.542(3)$ fm, giving a scattering length contrast of 0.106(3) fm between $^{13}$C and $^{\mathrm{nat}}$C. This contrast is about a factor of four smaller than the 0.46(9) fm expected from standard tables, and is consistent with the results of attempted NDIS studies mentioned above.

Our neutron diffraction experiments on liquid $^{13}CS_2$ and $^{\mathrm{nat}}CS_2$, and on liquid $^{13}CO_2$ and $^{12}CO_2$, lead to a value of $b_{\mathrm{incoh,13C}} = -0.42 \pm 0.24$ fm that is consistent with the standard tabulated value of $-0.52 \pm 0.09$ fm, and very close to the theoretical result of $-0.4$ fm. The accuracy of our diffraction results is limited by the purity of the $^{13}CS_2$ sample, and by knowledge of the molecular density of $^{13}CO_2$, as compared to $^{12}CO_2$, relatively close to the critical point.

By combining our neutron diffraction data with x-ray diffraction data, and making use of our value for $b_{\mathrm{coh,13C}} = 6.542(3)$ fm, we have also been able to determine the partial structure factors of liquid $CS_2$ and liquid $CO_2$, which will be reported elsewhere (Neuefeind *et al* 2008).

## 2. Neutron interferometry experiment to measure $b_{\mathrm{coh,13C}}$

Neutron interferometry (e.g. Rauch and Werner 2000) is analogous to photon interferometry, and provides a very precise method for measuring coherent scattering lengths. Note that neutron interferometry involves quantum mechanical correlations between particle wavefunctions separated by macroscopic distances (several cm) that are much larger than neutron coherence lengths of order 1 $\mu$m. A schematic of the technique is illustrated in figure 1. The presence of the samples induces a phase difference $\Delta\phi$ between the two components of the neutron's split wavefunction. This $\Delta\phi$ can be revealed by plotting the counting rate of the O or H detector as a function of an additional phase shift that has a nearly linear dependence on a small change in the phase-shifter angle $\delta$ (Rauch and Werner 2000, equation (2.7)). At each angle $\delta$ in the phase-shifter scan, the counts of the two detectors are measured with both samples raised above the interferometer (samples OUT), and with both samples precisely lowered into place (samples IN). Two sinusoidal curves are thereby generated for each detector and show a relative phase difference of $\Delta\phi$ for samples IN versus samples OUT. Note that the O and H detector counts are always 180° out of phase in $\phi$ with respect to each other, due to conservation of probability (since a given neutron is captured by exactly one or the other detector). A phase-shifter made of

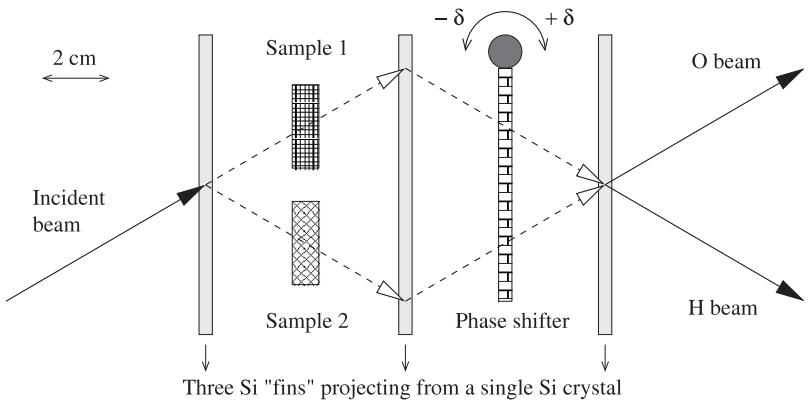


**Figure 1.** Schematic of a neutron interferometer, cut from a single boule of a perfect Si crystal. The incident neutron's wavefunction is split by the first Si 'fin' into a transmitted (O) and a diffracted (H) component. The two samples modify differently the optical path lengths of the two wavefunction components, which thereby accumulate a relative phase difference $\Delta\phi$ that affects their interference when recombined at the third Si fin. A phase-shifter of variable angle $\delta$ induces an additional phase shift between the two paths of the split wavefunction. The detected counting rates of the exiting O and H beams, measured as a function of the phase-shifter angle with and without the samples in position, allow $\Delta\phi$ to be determined.

Si monocrystal, as was the case for our experiment, need be rotated only a few degrees in physical angle $\delta$ in order to cover $4\pi$ (i.e. 2 periods) in $\phi$. The counting rates of the detectors can be as high as 1 kHz, and several phase-shifter scans are generally performed in order to increase statistics.

The measured phase difference $\Delta\phi$ (in radians) between the samples IN and OUT is directly proportional to the difference in optical path between the two trajectories of the split wavefunction, and therefore directly proportional to the difference in average (i.e. coherent) scattering length $\Delta\overline{b}$ between two samples of identical thickness:

$$\Delta\phi = n\lambda D\Delta\overline{b}, \tag{2.1}$$

where $\lambda$ is the neutron wavelength, $n$ the atomic number density and $D$ the sample thickness measured along the paths of the split wavefunction. Of course it is possible for one sample to be void, and then $\Delta\phi$ corresponds to the phase difference induced by the single sample used. However, a differential measurement between two samples, one having known scattering lengths, generally offers much greater precision in determining an unknown scattering length in the other sample. We therefore performed a differential measurement comparing $^{nat}CS_2$ and $^{13}CS_2$ samples.

### *2.1. Interferometry measurements on liquid $CS_2$*

The high-purity $^{nat}CS_2$ (>99.9% $CS_2$, <1 ppm benzene) was purchased from Sigma-Aldrich. Isotopically enriched $^{13}CS_2$ (97–99% $^{13}C$) was purchased from Cambridge Isotopes (MA, USA) in sealed 1 g vials. Although we have no information on the chemical purity of the $^{13}CS_2$ sample, one would expect some benzene contamination, since chemical purity is harder to achieve when producing small quantities of isotopically enriched samples.

We carried out our interferometry measurements at the S18 neutron interferometer (e.g. Kroupa *et al* 2000) of the Institut Laue-Langevin (ILL) in Grenoble, France. We used a perfect Si crystal interferometer of skew-symmetric geometry, which allows parallel samples to be placed perpendicular to both paths of the split wavefunction. Figure 2 shows typical interferometry data from our S18 experiment.

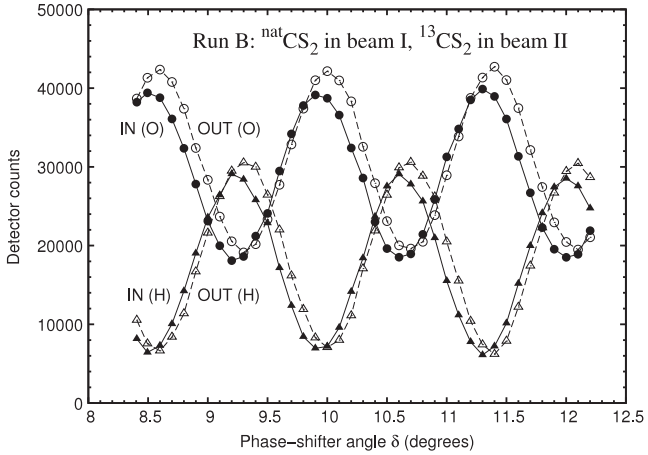


**Figure 2.** Neutron interferometry data for a typical phase-shifter scan, in this case part of run 'B', having $^{nat}CS_2$ mounted in the 'beam I' leg of the interferometer and $^{13}CS_2$ mounted in beam II. The counts of the O and H detectors (acquisition time: 30 s per point) are shown as a function of phase-shifter angle for samples IN (solid symbols) and samples OUT (open symbols). Fits to the sine curves give an IN–OUT phase difference of $\Delta\phi_B = -18.00° \pm 0.10°$ as averaged over the scans of run B, as compared to an empty-cell phase difference measured in another run to be $\Delta\phi_{B,empty} = -1.88° \pm 0.22°$. Note that the abscissa here represents the physical angle $\delta$ of the Si monocrystal phase-shifter in degrees, whose relation to $\phi$ is not perfectly linear and has been duly taken into account in the data analysis.

The neutron wavelength from the Si(220) monochromator reflection was measured via diffraction from a single-crystal Si sample at both dispersive and non-dispersive angles, and found to be $\lambda = 1.9233(10)$ Å. The $\lambda/2$ contamination at this wavelength is about 3% but does not affect the measured phase difference $\Delta\phi$, and therefore nor the determined coherent

scattering length, since the detector counting rate oscillations in $\phi$ coming from $\lambda/2$ are synchronous with those from $\lambda$ and merely have twice the period in $\phi$, so that each second maximum is slightly reduced in amplitude.

The temperature of the closed room housing the interferometer was measured to be 20.2 °C (293.35 K) at one point during the differential measurements comparing $^{nat}CS_2$ and $^{13}CS_2$ samples. By fitting a quadratic polynomial to reported data for the mass density of $CS_2$ as a function of temperature (Garcia Baonza *et al* 1989, Mopsik 1969), we find $\rho = 1.2632$ g cm$^{-3}$ at 20.2 °C, with an estimated uncertainty of less than 0.001 g cm$^{-3}$. An estimated temperature uncertainty of 1 °C implies however an additional density uncertainty of 0.0014 g cm$^{-3}$. Our atomic number density is then $n = 0.029\,97(4)$ Å$^{-3}$ at 20.2 °C, which we assume to be the same for the $^{nat}CS_2$ and $^{13}CS_2$ samples.

Each $CS_2$ sample was contained in a Hellma cell (type 404 QS) equipped with two Teflon stoppers. The interior thickness $D$ of the Hellma cells was quoted as 1.00(1) mm (Weill 2007), whose 1% uncertainty is a principal limitation in the precision of our measured scattering length difference $\Delta\overline{b}$. The two Hellma cells were thoroughly rinsed in acetone under ultrasound, with care taken not to soil or abrade their optically flat surfaces (gloves worn). We distinguished the two cells, one used for $^{nat}CS_2$ and the other for $^{13}CS_2$. Enough of each sample was available to fill the ∼0.7 cm$^3$ cell volume. Only a minute portion of each sample evaporated across the Teflon stoppers over a 24 h period (estimate $\lesssim$0.1%).

The two cells were slid horizontally into suspended position along a slot cut into a specially made Al sample holder, and then gently fixed in place with set screws. The sample holder was in turn suspended from an $x$–$y$–$z$ translation stage also permitting rotation about a vertical axis. A standard calibration procedure was used to fix the samples in the proper position and orientation. The sample cross-section in the cells was about 20 mm wide by 25 mm high, comfortably larger than the beam's cross-section of about 5 mm wide by 6 mm high.

### 2.2. Measurement of interior thickness difference between the two cells

Our differential interferometry measurement relies on the two Hellma cells having an identical interior thickness $D$, although this value of $D$ may differ from its nominal value of 1.00 mm. It is therefore necessary to measure accurately a possible difference $\Delta D$ in interior thickness between the two Hellma cells, which can be accomplished via photon absorption measurements on a suitable liquid sample. We used a UV–vis spectrophotometer that allows a simultaneous comparative measurement of the absorption of two samples. The standard definition for absorption,

$$\text{absorption} = -\log_{10}(I/I_0), \tag{2.2}$$

where $I_0$ and $I$ are the incident and transmitted photon intensities, takes into account the exponential dependence on thickness. One can therefore measure the absorption of a liquid placed in a Hellma cell by subtracting the absorption of the empty cell. Furthermore, it is clear that a small difference in absorption between two samples of the same material, divided by their nominal absorption, is equal to the interior thickness difference $\Delta D$ divided by the nominal interior thickness, whence

$$\Delta D = D \times \Delta\text{absorption}/\text{absorption}, \tag{2.3}$$

where in our case $D = 1.00(1)$ mm is the nominal interior thickness of our two Hellma cells, and therefore $\Delta D$ is the interior thickness difference of interest. For our photon absorption sample, we used a 1:200 $KMnO_4$ aqueous solution, since it manifests a convenient range of photon absorption over a relatively narrow wavelength range. The two Hellma cells were filled from the same syringe loading, one immediately after the other, and then sealed, in order to assure identical absorptivities of the $KMnO_4$ solution. The two filled cells were placed in the two sample positions of the spectrophotometer for a comparative absorption measurement to deduce Δabsorption, and then the two cell positions were exchanged, and an average was taken to eliminate systematic errors between the two sample positions (we found that there was a ∼1% systematic error in transmitted intensity between the two sample positions). Empty cell runs were performed for both configurations, as well as a background or 'baseline' run for the empty spectrophotometer. Care was taken to assure parallel alignment of the two cells, and the entire experiment was repeated to confirm reproducibility.

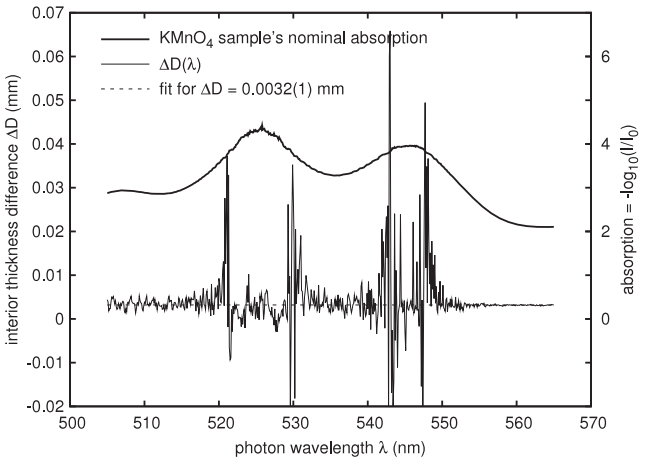


**Figure 3.** Measured photon absorption for a 1:200 $KMnO_4$ aqueous solution placed in the Hellma cells used for the neutron interferometry experiment. The best fit indicates an interior thickness difference of 3.2 ± 0.1 $\mu$m, i.e. 0.32%, between the two Hellma cells.

Figure 3 shows our spectrophotometer results. We found that the Hellma cell used for the $^{nat}CS_2$ sample in the S18 experiment has a *larger* interior thickness by 3.2(1) $\mu$m, which represents only 0.32% of the nominal interior thickness, but results in a non-negligible correction to our neutron interferometry results.

### 2.3. Interferometry results and discussion

There can remain an additional small systematic error in optical path due to the sample holder presenting slightly

different orientations for the two Hellma cell positions, nominally perpendicular to the two trajectories of the split wavefunction. We therefore performed two runs wherein the two samples, each contained in its own Hellma cell, switched positions between the two paths or legs (called beam I and beam II) of the interferometer. We arbitrarily named run A to be $^{13}CS_2$ in beam I and $^{nat}CS_2$ in beam II (resulting in $\Delta\phi > 0$), with run B being the other way around. Empty cell runs were likewise performed for the A and B configurations. One run consisted of about 20–25 phase-shifter scans, each lasting about 45 min, allowing the completion of about one run per day.

When sliding the cells in and out of the sample holder for loading, emptying and switching purposes, care was taken to reproduce accurately the cell positions. We obtained the following results for the measured phase differences in the A and B runs:

$$\Delta\phi_A = +17.20(11)^\circ \qquad \text{with } \Delta\phi_{A,empty} = +1.56(13)^\circ$$

$$\Delta\phi_B = -18.00(10)^\circ \qquad \text{with } \Delta\phi_{B,empty} = -1.88(22)^\circ$$

leading to an average phase difference $\Delta\phi_{avr}$ induced by the presence of the $^{13}CS_2$ and $^{nat}CS_2$ samples,

$$\begin{aligned}\Delta\phi_{avr} &= \tfrac{1}{2}[(\Delta\phi_A - \Delta\phi_{A,empty}) - (\Delta\phi_B - \Delta\phi_{B,empty})] \\ &= 15.88(15)^\circ = 0.2772(26)\ \text{rad}\end{aligned}$$

which has a fractional uncertainty of only about 1% and is independent of the small A/B-dependent systematic phase shift $\Delta\phi_{A/B} \approx \pm 0.25^\circ$. In addition, since empty cells were present in both beams I and II, any correction for air and humidity within the open cells will cancel in this case.

As described later, we determined that the extra 3.2(1) $\mu$m of thickness for the $^{nat}CS_2$ sample leads to an extra phase shift of $\Delta\phi_{extra} = 0.0753(24)$ rad or $4.31(13)^\circ$, which must therefore be subtracted from the value for $\Delta\phi_{avr}$, giving the corrected value for $\Delta\phi$ (note that $\Delta\phi_{avr}$ and $\Delta\phi_{extra}$ have comparable experimental uncertainties):

$$\begin{aligned}\Delta\phi &= \Delta\phi_{avr} - \Delta\phi_{extra} \\ &= 0.2772(26)\ \text{rad} - 0.0753(24)\ \text{rad} \\ &= 0.2019(35)\ \text{rad} = 11.57(20)^\circ.\end{aligned}$$

By solving equation (2.1) for $\Delta\overline{b}$ and plugging in the values for $n$, $\lambda$ and $D$, we obtain

$$\begin{aligned}\Delta\overline{b} = \tfrac{1}{3}(\overline{b}_{natC} - \overline{b}_{13C}) &= \Delta\phi/(n\lambda D) \\ &= \Delta\phi \times 0.1735(18)\ \text{fm}, \qquad (2.4)\end{aligned}$$

where $\overline{b}_{natC} = 6.6484(13)$ fm as tabulated by Rauch and Waschkowski (2002). The factor of one-third arises since C accounts for exactly one-third of the atoms in the $CS_2$ molecule. The roughly 1% uncertainty in the coefficient of $\Delta\phi$ stems almost entirely from the uncertainty in the Hellma cell nominal interior thickness.

The measured $\Delta\phi = 0.2019(35)$ then gives a value of 6.543(2) fm for the apparent average $^{13}C$ scattering length. However, as discussed in section 3.5 below, our diffraction results showed that the $^{13}CS_2$ sample was contaminated with an H-containing compound equivalent to about 345 ppm of benzene, which reduced slightly the sample's average scattering length density in the interferometry experiment. By correcting for this small effect, we obtain

$$\overline{b}_{C\ in\ 13CS2} = 6.544 \pm 0.002\ \text{fm}$$

for the average scattering length of the C atoms in the $^{13}CS_2$ sample. Now taking into account the estimated isotopic purity of 98(1)% $^{13}C$ as quoted by Cambridge Isotopes, we derive our final result for the bound coherent scattering length of $^{13}C$:

$$b_{coh,13C} = 6.542 \pm 0.003\ \text{fm},$$

which differs, beyond estimated experimental uncertainties, from the standard tabulated value of $6.19 \pm 0.09$ fm.

The $^{13}CO_2$ sample used in our diffraction experiments had an estimated isotopic purity of 99(1)% $^{13}C$, which leads to an average scattering length of 6.543(3) fm for its C atoms. Since this is equal, within experimental uncertainty, to the above value of 6.544(2) fm for the C atoms in the $^{13}CS_2$ sample, and in the interest of simplicity, we have chosen to use 6.543(3) fm as the average scattering length $\overline{b}_{13C}$ of the C atoms when analyzing the diffraction data for both the $^{13}CS_2$ and $^{13}CO_2$ samples (see table 1). This value of 6.543(3) fm corresponds to a 98.9% isotopic purity for $^{13}C$, which is consistent with the quoted isotopic purities of both our $^{13}CS_2$ and $^{13}CO_2$ samples. Note that a change of 0.001 fm in $\overline{b}_{13C}$ engenders a change of about 0.015 fm in $b_{incoh,13C}$ as derived from the diffraction data analysis.

Using again the precisely known coherent scattering length 6.6484(13) fm of $^{nat}C$, along with our result of $b_{coh,13C} = 6.542(3)$ fm, we can obtain a more accurate value for the bound coherent scattering length of $^{12}C$:

$$b_{coh,12C} = 6.6496 \pm 0.0013\ \text{fm},$$

as compared to the standard tabulated value of 6.6535(14) fm.

The neutron scattering length contrast is therefore only 0.108(3) fm between $^{13}C$ and $^{12}C$, and only 0.106(3) fm between $^{13}C$ and $^{nat}C$, which makes isotopic substitution experiments on carbon particularly challenging.

**Table 1.** Coherent and incoherent scattering lengths used in the analysis of the $CS_2$ and $CO_2$ diffraction data, including the MD simulations. The $b_{incoh}$ of the natural 'isotopes' is derived from the incoherent scattering lengths of the component isotopes and the variance of their coherent scattering lengths: $\text{var}(b) = \overline{b^2} - \overline{b}^2$. For simplicity, here we assign absolute values to all $b_{incoh}$ (see section 3.7). Note that the value listed here for $b_{coh,13C}$ differs from our final value of 6.542(3) fm since it takes into account the isotopic purity of the $^{13}CS_2$ and $^{13}CO_2$ samples. A change of 0.001 fm in $b_{coh,13C}$ engenders a change of about 0.015 fm in the value of $b_{incoh,13C} = 0.42(24)$ fm derived from our diffraction data, listed here for completeness.

| Isotope | $b_{coh}$ (fm) | $b_{incoh}$ (fm) | Source |
|---|---|---|---|
| $^{nat}S$ | 2.847(1) | 0.24(8) | Sears (1992) |
| $^{nat}O$ | 5.805(4) | 0.0(2) | Rauch and Waschkowski (2002) |
| $^{nat}C$ | 6.6484(13) | 0.09(18) | Rauch and Waschkowski (2002) |
| $^{12}C$ | 6.6496(13) | 0.0 | This work |
| $^{13}C$ | 6.543(3) | 0.42(24) | This work |

In order to determine the aforementioned extra phase shift coming from the extra 3.2 $\mu$m interior thickness of the Hellma cell used for the $^{nat}CS_2$ sample, we needed an absolute measurement of the total phase difference induced by the $^{nat}CS_2$ sample alone. This absolute measurement will also provide a value for $b_{coh,natC}$ (although with much less precision than for a differential measurement as described above) that can be compared to the very precise tabulated value for $b_{coh,natC}$, thereby confirming that there were no unknown significant systematic errors involved in our interferometry experiment.

We therefore performed a run (A configuration) on $^{nat}CS_2$ in its cell in one leg versus $^{13}CS_2$'s empty cell in the other leg, which allows $\overline{b}_{natC} = b_{coh,natC}$ to be measured, where we make use of the tabulated value $b_{coh,S} = 2.847(1)$ fm for sulfur's coherent scattering length. Duly subtracting $\Delta\phi_{A,empty}$ and including the small A-dependent systematic phase shift mentioned above, as well as a small correction for 992 mbar of air and 40% relative humidity in the open empty cell (Rauch and Werner 2000, section 3.4.1), we measured a phase difference of 23.5261(46) rad = 267.95(26)°+3·360° induced by the $^{nat}CS_2$ sample alone.

The extra phase shift resulting from the 3.2(1) $\mu$m extra interior thickness is thus 23.5261(46) · 3.2/1000 = $\Delta\phi_{extra} = 0.0753(24)$ rad or 4.31(13)°, assuming 1.00 mm as the nominal interior thickness. This result represents 0.0753/0.2772 ∼ 27% of the uncorrected phase difference between the $^{nat}CS_2$ and $^{13}CS_2$ samples, and is therefore a significant systematic correction.

During this absolute measurement on $^{nat}CS_2$, the temperature in the interferometer room was measured to be 22(1) °C, giving an atomic number density of $n = 0.029\,90(4)$ Å$^{-3}$ for the sample. The derived coherent scattering length for $^{nat}C$ is then 6.58(12) fm (again assuming 1.00 mm as the nominal interior thickness), which agrees within experimental uncertainty with the standard tabulated value of $b_{coh,natC} = 6.6484(13)$ fm. Note that the ±0.12 fm precision in our result for $b_{coh,natC}$ is in fact larger than the scattering length contrast between $^{nat}C$ and $^{13}C$, demonstrating clearly the advantage of performing a differential interferometry measurement using both $^{nat}CS_2$ and $^{13}CS_2$ samples.

## 3. Neutron diffraction experiments to measure $b_{incoh,13C}$

Neutron diffraction makes no analysis of the scattered neutron energy at detection, and therefore measures the *total scattering* differential cross-section per atom, $d\sigma/d\Omega$, that can be expressed as the sum of two terms:

$$\left[\frac{d\sigma}{d\Omega}(Q)\right] = \left[\frac{d\sigma}{d\Omega}(Q)\right]_{distinct} + \left[\frac{d\sigma}{d\Omega}(Q)\right]_{self} \qquad (3.1)$$

where $Q = (4\pi/\lambda)\sin(2\theta)$ is the neutron wavevector transfer at diffraction angle $2\theta$ and neutron wavelength $\lambda$. The so-called distinct term results from scattered wave interference between distinct atoms in the sample, depends only on the coherent scattering lengths, and carries all information about the sample's structure. Although the measured total scattering intensity must be positive definite, the distinct scattering contribution can be negative.

As $Q \to \infty$ and the scattered waves from distinct atoms lose phase correlation, the distinct term approaches zero intensity, and thus the measured $d\sigma/d\Omega$ approaches the value of the second term in equation (3.1). This asymptotic intensity is called the *self-scattering* as it represents the isotopically scattered intensity $b^2$ from each atom individually, without interference between atoms, and then averaged over all the sample's atoms. The self-term's only $Q$-dependence stems from inelasticity effects (Placzek 1952, Yarnell *et al* 1973), that cause a 'Placzek falloff' of intensity according to a polynomial of even powers in $Q$:

$$\left[\frac{d\sigma}{d\Omega}(Q)\right]_{self} = \overline{b^2}\left[1 + P_2Q^2 + P_4Q^4 + \cdots\right] \qquad (3.2)$$

where the Placzek coefficients $P_n$ depend on the masses of the sample's atoms, and where the $Q^4$ and higher terms can generally be neglected for atomic masses above 20 amu. The self-scattering intensity can therefore be extracted from neutron diffraction data by fitting the total scattering $d\sigma/d\Omega$ to a polynomial of even powers in $Q$. The distinct scattering will simply contribute oscillations about this fit. The $Q = 0$ limit of the measured self-scattering can then be expressed as an average over all $N$ isotopes $i$ having known concentrations $c_i$ in the sample ($\Sigma c_i = 1$):

$$\overline{b^2} = \sum_{i=1}^{N} c_i\overline{b_i^2} \qquad \text{and} \qquad \overline{b_i^2} = b_{coh,i}^2 + b_{incoh,i}^2, \qquad (3.3)$$

where $b_{coh,i} = \overline{b}_i$ per usual. When all scattering lengths are known, except for example $b_{incoh,13C}^2$, the latter can be determined from diffraction data. Note that our technique of unpolarized neutron diffraction provides only $b_{incoh}^2$ and therefore cannot resolve the sign of $b_{incoh}$, for which a neutron polarization experiment is necessary (see section 3.7). For the moment, we will consider $b_{incoh}$ to represent an absolute value of the incoherent scattering length, in the interest of simplicity. Table 1 lists the values of $b_{coh,i}$ and $b_{incoh,i}$ that we used for analysis of our diffraction data.

Since the scattering lengths of $^{nat}C$, $^{12}C$ and $^{13}C$ are very similar, our measured diffraction patterns for $CS_2$ and $CO_2$ will show only a small change from isotopic substitution. In order to aid the cancelation of possible systematic errors, it is thus advantageous to take the ratio of the measured diffraction intensities or diffractograms. Moreover, the diffractogram ratio will manifest smaller-amplitude oscillations coming from the distinct scattering, permitting a more robust fit to the self-scattering ratio, expressed for two samples 'A' and 'B' as

$$R_{self}(Q) = \frac{\overline{b^2}_A\left[1 + P_{2,A}Q^2 + P_{4,A}Q^4 + \cdots\right]}{\overline{b^2}_B\left[1 + P_{2,B}Q^2 + P_{4,B}Q^4 + \cdots\right]} \qquad (3.4)$$

which to first order in $Q^2$ becomes

$$R_{self}(Q) = (\overline{b^2}_A/\overline{b^2}_B)\left[1 + (P_{2,A} - P_{2,B})Q^2 + \cdots\right]. \qquad (3.5)$$

Note that the resulting amplitude of the Placzek falloff is weighted by the ratio in self-scattering intensities: $\overline{b^2}_{\mathrm{A}}/\overline{b^2}_{\mathrm{B}}$. The fit to $R(Q)$ can be evaluated at $Q = 0$, to which

$$R_{\mathrm{self}}(0) = \frac{\sum c_{i,\mathrm{A}}(b^2_{\mathrm{coh},i,\mathrm{A}} + b^2_{\mathrm{incoh},i,\mathrm{A}})}{\sum c_{i,\mathrm{B}}(b^2_{\mathrm{coh},i,\mathrm{B}} + b^2_{\mathrm{incoh},i,\mathrm{B}})}, \qquad (3.6)$$

where the sums run over all isotopes and nuclear spin states of the two samples, supposed for our purposes to be of identical chemical composition. A precise measurement of $R_{\mathrm{self}}(0)$ then allows equation (3.6) to be solved for an unknown scattering length, in our case $b^2_{\mathrm{incoh,13C}}$.

To calculate the experimental uncertainties in derived results, such as that for $b_{\mathrm{incoh,13C}}$ derived from the diffraction data, we have used standard error-propagation techniques via evaluation of the differential $\mathrm{d}F$ for a function $F$ of several variables, where the experimental uncertainties in these input variables are assumed to be uncorrelated. For simplicity, we have chosen to quote the experimental uncertainties in derived results as symmetric ($\pm\mathrm{d}F$) rather than asymmetric ($-\mathrm{d}F_{\mathrm{lower}}/+\mathrm{d}F_{\mathrm{upper}}$).

A good fit to $R_{\mathrm{self}}(Q)$ requires a sufficiently large range in $Q$, whence the advantage of using short-wavelength or 'hot' neutrons. Our diffraction experiments were carried out at the liquid diffractometer D4c (Fischer *et al* 2002) mounted on the hot neutron source of the high-flux reactor at the Institut Laue–Langevin (ILL) in Grenoble, France. The incident neutron wavelength of about 0.5 Å provided $Q_{\mathrm{max}} \approx 23.5$ Å$^{-1}$. D4c is the ideal instrument for precise measurements of total scattering intensity, having a counting rate stability of about $2 \times 10^{-4}$ over three days, and a reproducibility in measured diffraction intensity (for a given sample) of about $10^{-3}$. The accuracy of measurements at D4c is generally limited by the sample quality/purity and by the precision of the sample mounting/environment, not by the instrument itself.

Sections 3.1–3.3 describe the experimental method and instrument characterization for our diffraction measurements. Sections 3.4–3.6 discuss the analysis procedure for the $CO_2$ and $CS_2$ diffraction data, which led to a value for $b_{\mathrm{incoh,13C}}$ that is consistent with both data sets. The accuracy of our obtained value $b_{\mathrm{incoh,13C}} = -0.42(24)$ fm is however limited by an uncertainty in the amount of benzene contamination in the $^{13}CS_2$ sample, and by an uncertainty in $^{13}CO_2$'s molecular number density near the critical point. Finally, section 3.7 discusses the spin-dependent scattering lengths of $^{13}$C and why the sign of $b_{\mathrm{incoh,13C}}$ is negative.

### *3.1. Diffraction data for liquid $CS_2$*

The same Helicoflex-sealed vanadium can (5.0 mm i.d./5.2 mm o.d.) was used for both $^{13}CS_2$ and $^{\mathrm{nat}}CS_2$ samples. In order to minimize any difference in multiple scattering between the two samples, we filled each to the same height of about 40 mm, using a syringe under a fume hood. As $CS_2$ has a very high vapor pressure, we weighed each sample (while sealed in the can) before and after its data runs, which showed no mass loss within ±0.01 g. Gloves were worn to avoid contaminating the outside of the can with H-containing compounds. Each sample was mounted in the D4c vacuum vessel or bell-jar by screwing the can's bottom onto an M4 bolt atop the standard 'candlestick' fixed rigidly in place. Dismounting and remounting of samples involved only the screwing/un-screwing of this M4 thread, which assured the same orientation of the sample can each time. Vertical beam-defining slits, made of $^{10}B_4C$, were placed a few centimeters upstream of the sample to produce a beam height of 30 mm centered on the sample height.

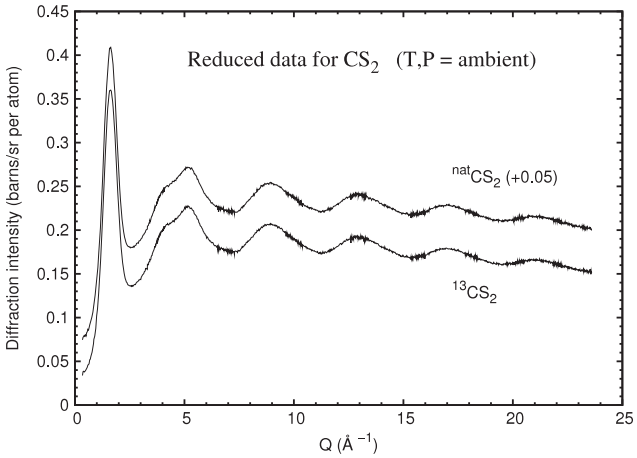


**Figure 4.** Neutron diffraction data for liquid $CS_2$ after subtraction of background and vanadium container scattering, as well as corrections for multiple scattering and attenuation. The apparent extra statistical noise at the detector overlap regions is simply due to the type of Q-binning used.

Data acquisition was organized in several (about ten) scans of about 1 h duration each in order to compare successive scans for stability checks. The temperature of the sample support (about 20 cm from the sample) was measured with a thermocouple inside the vacuum vessel. This temperature would drop by about 1 K immediately after pumping, and then over the next 20 min regain the stable range of 300.45 ± 0.1 K that persisted over the three days of the experiment. As described in section 2.1, we calculate a molecular density of 0.009 905(5) Å$^{-3}$ for $CS_2$ at 300.45 K.

The neutron wavelength was measured to be 0.4977(2) Å using a standard Ni powder sample. Diffractograms were also acquired for the empty bell-jar and the empty can, as well as a vanadium standard for intensity calibration. Standard software (Howe *et al* 1998) was used to correct the diffraction data for attenuation and multiple scattering, as well as to subtract properly the scattered intensities from background and empty container. Figure 4 shows our reduced diffraction data for both $^{13}CS_2$ and $^{\mathrm{nat}}CS_2$ samples.

### *3.2. Stability and reproducibility of the diffraction measurements*

Since we needed to measure very small differences between the diffraction intensities of the $^{13}CS_2$ and $^{\mathrm{nat}}CS_2$ samples, it was necessary to confirm the stability and reproducibility of the diffractograms as measured by the D4c instrument. The counting rate stability of D4c during a given sample mounting

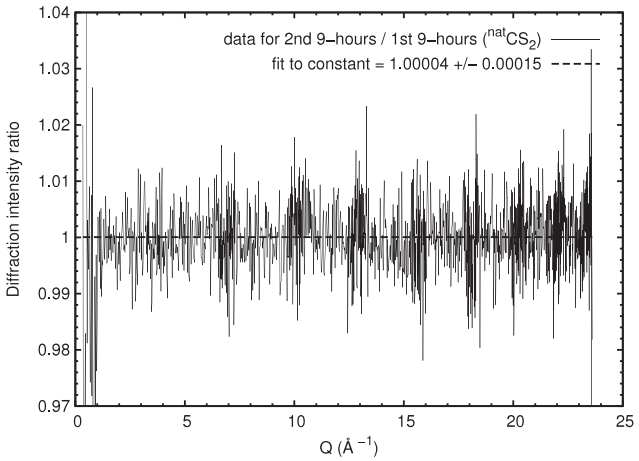


**Figure 5.** Measured counting rate stability of the D4c diffractometer, obtained for the liquid $^{nat}CS_2$ sample by dividing the second half of an 18 h acquisition by the first half. This measured stability of $(0.4 \pm 1.5) \times 10^{-4}$ over 9 h is consistent with the instrument's quoted stability of $2 \times 10^{-4}$ over three days.

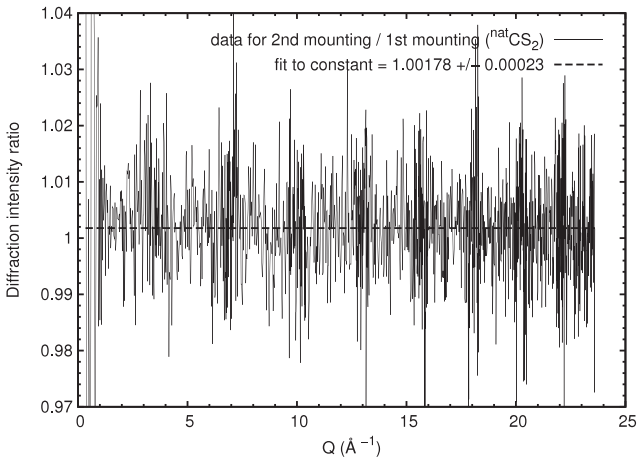


**Figure 6.** Measured diffractogram reproducibility of the D4c diffractometer, obtained for the liquid $^{nat}CS_2$ sample by remounting the same sample and dividing a 2 h acquisition by the original 18 h acquisition. The obtained reproducibility of $(17.8 \pm 2.3) \times 10^{-4}$ is consistent with previous experience in using this diffractometer.

is quoted as $2 \times 10^{-4}$ over three days (Fischer *et al* 2002), which does not take into account possible variations in the sample (e.g. temperature) during data acquisition. The reproducibility of a diffractogram between two mountings of a given sample is generally of order $10^{-3}$, depending on the nature of the sample mounting.

Figures 5 and 6 show respectively the counting rate stability and diffractogram reproducibility that we measured during the $CS_2$ diffraction experiments. The results conform to past experience with the instrument's performance, and are sufficiently good for the present diffraction study. These experimental uncertainties were nevertheless duly incorporated into the analysis of our diffraction data.

### *3.3. Diffraction data for liquid $CO_2$*

Bottled samples of isotopically enriched $^{13}CO_2$ (>98% $^{13}C$, <1% $^{18}O$) and $^{12}CO_2$ (99.95% $^{12}C$) were purchased from Cambridge Isotopes (MA, USA). The isotopic compositions of the $CO_2$ samples were checked by mass spectroscopy and found to agree with specifications. As mentioned earlier, in our data analysis we have used the value 98.9% $^{13}C$ for the isotopic composition of the $^{13}CO_2$ sample, resulting in the value for $b_{coh,13C}$ shown in table 1. Using appropriate gas handling equipment, the samples were loaded from their bottles into a medium pressure aluminum cell that allows adjustment of temperature and pressure up to 333 K and 100 bar and has been described elsewhere (Neuefeind *et al* 2000). The $^{10}B_4C$ vertical beam-defining slits, placed a few centimeters upstream of the sample inside the D4c vacuum vessel or bell-jar, were set to 40 mm height.

To change samples it was necessary to dismount the pressure cell, recover the previous sample from the cell using $LN_2$ cryopumping, and then follow a dilution procedure of four successive fillings + ventings of the new sample into the cell, which reduced the possible contamination by the previous sample to less than $10^{-4}$. Care was taken to mount the cell in the same position after sample exchange: as discussed later, our data analysis showed that our sample-mounting precision was about 0.3 mm (horizontally), which was good enough to reproduce the sample volume illuminated by the beam, since the horizontal beam-defining slits were set sufficiently wide.

The experiments were carried out at a temperature of about 298 K and a pressure of about 66 bar, a state point in the liquid stability field of carbon dioxide. The temperature of the sample at the control thermocouple was very stable (within mK), but a temperature gradient across the cell of 0.3 K was measured, and we have estimated 298.1 K as the temperature at the center of the sample for all the data runs.

Due to a slow mechanical relaxation of our gas handling system (involving several meters of tubes and capillary) and perhaps also a very small leak, the measured pressure of the sample would decrease by 1 or 2 bar over a 24 h period. Data acquisition was organized in runs of several (about ten) scans of about 40 min duration to minimize the effect of pressure drifts. During the $^{13}CO_2$ run the pressure slowly decreased by 0.5 bar, resulting in an average of 65.32 bar. For the first $^{12}CO_2$ run, the downward drift was about 1.1 bar, for an average of 64.77 bar. The absolute accuracy of the pressure measurement is estimated to be not better than 0.2 bar, but since we used the same set-up for both samples possible systematic errors should cancel out.

Because returning to exactly the same state point with independently loaded samples is difficult, we performed a second run on $^{12}CO_2$ at a slightly (2.5 bar) higher average pressure of 67.28 bar (having downward drift of 0.3 bar), which corresponds to a 2.2% higher density (Span and Wagner 1996) as compared to the first $^{12}CO_2$ run. Since the average pressure of the $^{13}CO_2$ run was between those of the two for $^{12}CO_2$, an appropriate linear combination of the $^{12}CO_2$ diffractograms reproduced the 65.32 bar average pressure for the $^{13}CO_2$ diffractogram.

We could thus compare the $^{12}CO_2$ and $^{13}CO_2$ samples at the same theoretical state point of $T = 298.1$ K and

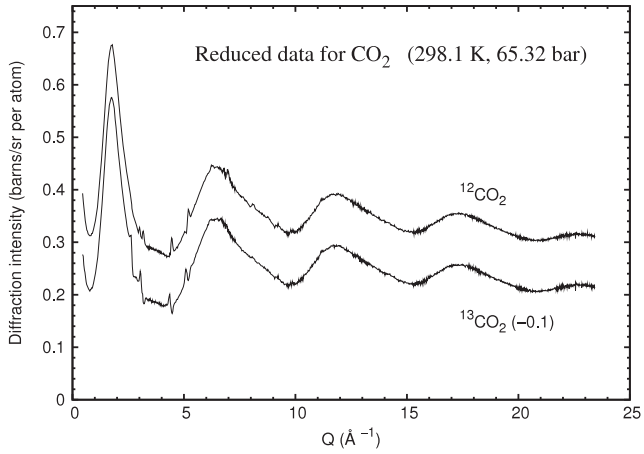


**Figure 7.** Neutron diffraction data for liquid $CO_2$ at 298.1 K and 65.32 bar average pressure, after subtraction of background and aluminum pressure cell scattering, as well as corrections for multiple scattering and attenuation. Although the cell was pressurized with weakly scattering argon for the empty cell run, the subtraction of the pressure-dependent Al Bragg peaks is not perfect (∼1% remaining intensity), due to a sample-position reproducibility of only ∼0.3 mm, as well as some strain hysteresis.

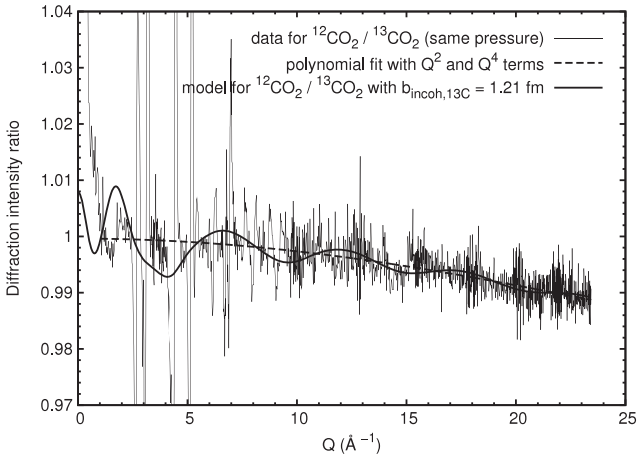


**Figure 8.** Ratio of $CO_2$ diffractograms shown in figure 7. The Placzek falloff is well fitted by a constant plus $Q^2$ and $Q^4$ terms, giving a $Q = 0$ intercept of $R_{self}(0) = 0.999\,62(24)$ and thence a value of 1.21(25) fm for $b_{incoh,13C}$. However, the oscillation amplitudes of the corresponding $CO_2$ model ratio are too large compared to those of the data (ignoring the sharp S-shaped Bragg peak residuals).

$P = 65.32$ bar, for which the molecular density of $^{nat}CO_2$ is $n = 0.009\,838(2)$ Å$^{-3}$ (Span and Wagner 1996).

Since the intensities and positions of the Bragg peaks from the Al pressure cell are dependent on pressure, we performed scans for the cell pressurized with weakly scattering Ar, serving as an 'empty cell' diffractogram, in addition to empty bell-jar scans. The same flushing procedure was used to remove the Ar sample before loading the $^{12}CO_2$ sample, and later mass spectrometer analysis of the recovered $^{12}CO_2$ sample showed no (i.e. <0.1%) contamination by Ar. No vanadium standard was run, and the data for the two $CO_2$ samples were normalized by the same constant to produce diffractograms conforming to their respective self-scatterings. The neutron wavelength was measured to be 0.5021(2) Å using a standard Ni powder sample. As for the $CS_2$ diffraction experiments, the same software (Howe *et al* 1998) was used to correct the diffraction data for attenuation and multiple scattering, as well as background and empty container subtraction. Figure 7 shows our reduced diffraction data for both $^{13}CO_2$ and $^{12}CO_2$ samples.

### *3.4. Preliminary analysis of $CO_2$ diffraction data*

As described earlier, the measured diffractograms of the two $CO_2$ samples were divided in order to facilitate the extraction of their relative self-scattering intensities. Figure 8 shows the resulting diffractogram ratio for the data of figure 7 where the $^{12}CO_2$ and $^{13}CO_2$ samples were at the same pressure of 65.32 bar. We chose arbitrarily to divide always the $^{12}C$-containing sample by the $^{13}C$-containing sample, since the smaller mass of the $^{12}C$ isotope leads to an intensity ratio having a familiar Placzek decrease with increasing $Q$. The approximately 1% falloff of the Placzek fit shown in figure 8 is consistent with that expected from equation (3.5), taking into account the relative masses of the carbon isotopes. Applying equation (3.6) to the fitted $R_{self}(0)$ ratio of self-scattering intensities leads to an incoherent scattering length $b_{incoh,13C} = 1.21(25)$ fm, which is considerably larger than the standard value of 0.52(9) fm from Glättli *et al* (1979).

In a parallel work (Neuefeind *et al* 2008) we have used these same neutron diffraction data, coupled with x-ray diffraction data taken at the same $(T, P)$ state point, to determine partial structure factors that allow a refinement of pair potentials for $CO_2$ in molecular dynamics (MD) simulations. These simulations produce a structural model for $CO_2$ under our experimental conditions. We have then calculated the neutron diffraction patterns for $^{12}CO_2$ and $^{13}CO_2$ expected from this model using 1.21 fm for $b_{incoh,13C}$ as well as the other scattering lengths listed in table 1. The resulting model ratio is plotted in figure 8, and exhibits distinct-term oscillations that are considerably larger than those of the data ratio.

A smaller input value for $b_{incoh,13C}$, coming from a larger value of $R_{self}(0)$, leads to smaller oscillation amplitudes in the model ratio. However, the needed change in $R_{self}(0)$ is beyond the estimated reproducibility of our diffraction intensities. For example, we determined that the S-shaped Bragg peak residuals of the data ratio are due to a 0.3 mm horizontal shift in sample position between the $^{12}CO_2$ and $^{13}CO_2$ runs. This sample-mounting imprecision cannot however account for a significant change in the beam-illuminated pressure cell volume, since even a 0.1% change in its diffraction intensity greatly increases the integrated intensity of the Bragg peak ratio residuals, which should remain close to zero. Therefore, one cannot explain the obtained large value of $b_{incoh,13C} = 1.21(25)$ fm as due to a change in diffraction intensity from the pressure cell.

We conclude that this preliminary analysis of our $CO_2$ diffraction data produces a value for $b_{incoh,13C}$ that is

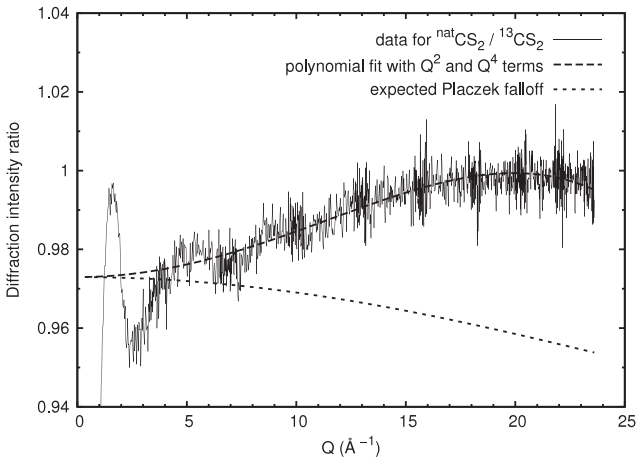


**Figure 9.** Ratio of $CS_2$ diffractograms shown in figure 4. A fit to the data ratio shows a strong divergence from the expected Placzek falloff derived from the $CO_2$ data ratio of figure 8, which is a sign of contamination by an H-containing compound in the $^{13}CS_2$ sample since its intensity appears in the denominator of the data ratio.

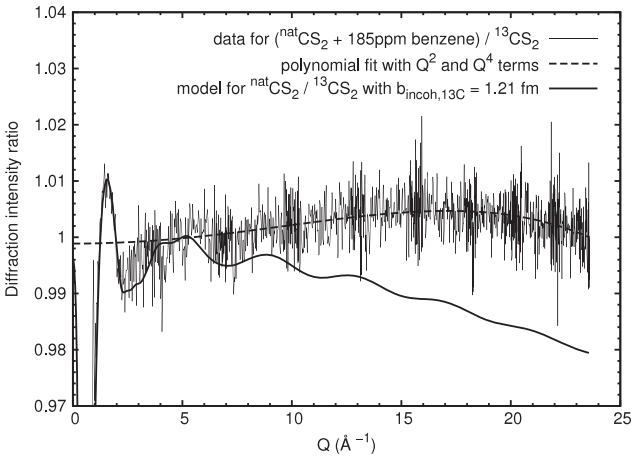


**Figure 10.** A diffractogram equivalent to a 185 ppm benzene contamination in the $^{nat}CS_2$ sample leads to a data ratio giving a $Q = 0$ intercept of $R_{self}(0) = 0.998\,87(24)$ and thence a value of 1.21(9) fm for $b_{incoh,13C}$, the same as obtained from the preliminary analysis of the $CO_2$ data. This 185 ppm data ratio does not however agree with the expected Placzek falloff included in the corresponding $CS_2$ model ratio.

considerably greater than the currently accepted value, and which leads to a model ratio showing distinct-term oscillations that are inconsistent with the data.

### *3.5. Analysis of $CS_2$ diffraction data*

Figure 9 shows the diffractogram ratio for the data of figure 4, where $^{nat}CS_2$ has been divided by $^{13}CS_2$. Also shown is the expected Placzek falloff from the carbon mass difference, calculated by scaling the $Q^2$ and $Q^4$ terms found for $^{12}CO_2/^{13}CO_2$ in figure 8 by the ratio of self-scatterings for $CS_2$ compared to $CO_2$ per equation (3.4), since S scatters considerably less than O. It is clear that the data ratio does not correspond at all to the expected Placzek falloff but diverges upwards with a shape that resembles an inverted version of the stronger Placzek falloff of hydrogen. This upturn strongly suggests contamination by an H-containing compound in the $^{13}CS_2$ sample since its intensity appears in the denominator. As mentioned earlier in section 2.1, benzene is a frequent contaminant in $CS_2$, and would be more difficult to eliminate from isotopically enriched samples that generally can be produced only in very small quantities.

We therefore prepared a sample of $^{nat}CS_2$ containing 1955 ppm of benzene and measured its diffractogram. By taking linear combinations with the diffractogram of the uncontaminated $^{nat}CS_2$, we can construct a $^{nat}CS_2$ diffractogram that reproduces the H-contamination of the $^{13}CS_2$ sample. The Placzek falloff of the data ratio should then conform to expectations. Even if the contaminant in the $^{13}CS_2$ is not benzene, the important factor is the amount of H in the sample, due to its very large incoherent scattering cross-section of 80.3 b that dominates the self-scattering of other atomic species. Obviously then, even a small amount of H can have an appreciable effect on the value of $R_{self}(0)$ obtained by fitting the data ratio.

Figure 10 shows a data ratio for which the equivalent amount of benzene in the $^{nat}CS_2$ has been adjusted to 185 ppm in order to produce an $R_{self}(0)$ that leads to the same value for $b_{incoh,13C}$ (here 1.21(9) fm) as that obtained from the $CO_2$ data ratio of figure 8. Also shown is the model ratio obtained for $b_{incoh,13C} = 1.21$ fm (and using table 1) from our molecular dynamics (MD) simulations of $CS_2$ (Neuefeind *et al* 2008) where we have included the expected Placzek effect. As was the case for $CO_2$, the MD simulations for $CS_2$ use pair potentials that have been refined with respect to the partial structure factors obtained by combining our $CS_2$ neutron diffraction data with x-ray diffraction data. Although the data ratio's oscillation amplitudes agree reasonably well with those of the model ratio in figure 10, there remains a significant departure from the Placzek falloff, which suggests that the equivalent benzene contamination of the $^{13}CS_2$ is greater than 185 ppm.

Figure 11 shows a data ratio for which the equivalent amount of benzene in the $^{nat}CS_2$ has been adjusted to 345 ppm in order to produce the expected Plazcek falloff in the data ratio. However, the fitted $R_{self}(0)$ intercept then leads to a value of 0.42(16) fm for $b_{incoh,13C}$, about a factor of three smaller than the value obtained from the preliminary analysis of the $CO_2$ data. Nevertheless, the model ratio for $b_{incoh,13C} =$ 0.42 fm exhibits oscillations that agree well with those of the 345 ppm data ratio, which constitutes a certain level of self-consistency in the result.

In order to test the sensitivity of our result for $b_{incoh,13C}$ to the precision of the Placzek fit to the data ratio, we refitted the $CO_2$ data ratio of figure 8 by using only a $Q^2$ term. We then found that an equivalent benzene contamination of 360 ppm would produce a data ratio for $CS_2$ whose $Q^2$ coefficient, when fitted with only a $Q^2$ term, matched that expected from the $CO_2$ data ratio. The resulting $R_{self}(0)$ for 360 ppm led to a value of 0.22(31) fm for $b_{incoh,13C}$, i.e. 0.2 fm smaller than that for 345 ppm fitted with both $Q^2$ and $Q^4$ terms. Although the inclusion of a $Q^4$ term cannot be firmly justified, we were

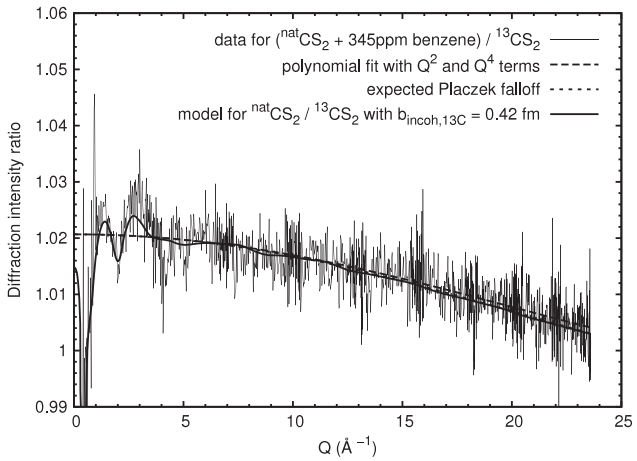


**Figure 11.** A diffractogram equivalent to a 345 ppm benzene contamination in the $^{nat}CS_2$ sample leads to a data ratio having the expected Placzek falloff. The fitted $Q = 0$ intercept of $R_{self}(0) = 1.020\,67(22)$ gives a value of 0.42(16) fm for $b_{incoh,13C}$, as compared to the 1.21(25) fm value resulting from the preliminary analysis of the $CO_2$ data. The oscillation amplitudes of this 345 ppm data ratio also conform well to those of the corresponding $CS_2$ model ratio.

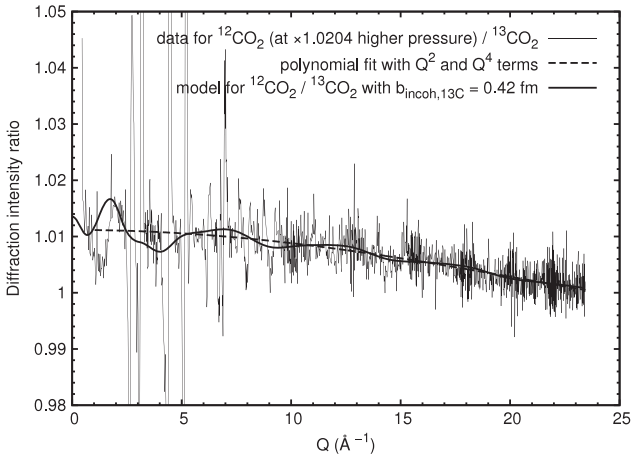


**Figure 12.** A diffractogram for $^{12}CO_2$ equivalent to a 2.04% higher average pressure (giving a 1.16% higher molecular density) leads to a data ratio having a $Q = 0$ intercept of $R_{self}(0) = 1.011\,17(26)$ and thence a value of 0.42(72) fm for $b_{incoh,13C}$ that agrees with the value of 0.42(24) fm obtained from the $CS_2$ data of figure 11. In addition, the oscillation amplitudes of this higher pressure data ratio are consistent with those of the corresponding $CO_2$ model ratio. The discrepancy in oscillation phase between data and model, occurring at 1–2 Å$^{-1}$, can be partially attributed to the 0.3 mm shift in sample position between the $^{12}CO_2$ and $^{13}CO_2$ runs. The fit to the Placzek falloff gives essentially the same $Q$ dependence as shown in figure 8.

impressed that adjustment of a single parameter (the ppm of benzene) allowed both the $Q^2$ and $Q^4$ coefficients to converge towards the values expected from the $CO_2$ data ratio. We therefore prefer to retain the Placzek fits using both a $Q^2$ and $Q^4$ term for the $CO_2$ and $CS_2$ data ratios, which leads to 345 ppm equivalent benzene and $b_{incoh,13C} = 0.42(16)$ fm as already described.

The 360 ppm result for $b_{incoh,13C}$ does however provide a good estimate for the uncertainty involved in 'tuning' the ppm level of equivalent benzene contamination, producing a change of 0.2 fm in $b_{incoh,13C}$ as compared to the value obtained by using 345 ppm. This 'ppm uncertainty' of ±15 ppm benzene turns out to be the largest contribution to the final ±0.24 fm uncertainty in the obtained bound incoherent scattering length of $^{13}C$ from the $CS_2$ diffraction data:

$$|b_{incoh,13C}| = 0.42 \pm 0.24 \text{ fm},$$

where we have included explicitly the absolute value signs, since our diffraction experiments cannot alone resolve the sign of $b_{incoh,13C}$ (see section 3.7 below). The second largest contribution to the uncertainty in $b_{incoh,13C}$ comes from the sample remounting precision of figure 6, for which a change of 0.001 78 in $R_{self}(0)$ leads to a change of 0.11 fm in $b_{incoh,13C}$. For comparison, the 0.003 fm uncertainty in the input value 6.543 fm for $b_{coh,13C}$ (see table 1) leads to a change of only 0.045 fm in $b_{incoh,13C}$.

### *3.6. Re-analysis of $CO_2$ diffraction data*

Recalling that $b_{incoh,13C} = 1.21$ fm did not lead to a model ratio that matched the data ratio for $^{12}CO_2/^{13}CO_2$, we generated a model ratio using the 0.42 fm value for $b_{incoh,13C}$ obtained in the $CS_2$ diffraction data analysis. Employing again the technique for linear combinations of the two $^{12}CO_2$ runs at different pressures, we constructed a $^{12}CO_2$ diffractogram equivalent to 2.04% higher pressure, giving a data ratio whose fitted $R_{self}(0)$ led to a value of 0.42(72) fm for $b_{incoh,13C}$. The resulting data ratio and model ratio are shown in figure 12. As compared to the earlier results of figure 8, here the model ratio oscillations have amplitudes that are consistent with those of the data. The small discrepancy in oscillation phase around 1–2 Å$^{-1}$ is partly explained by the 0.3 mm shift in sample position that we noted between the $^{12}CO_2$ and $^{13}CO_2$ runs. Note that the Placzek falloff is insensitive to the pressure increase, and its fit gives essentially the same $Q$ dependence as shown in figure 8.

It only remains to show that a 2.04% higher pressure for $^{12}CO_2$ is required to produce the same molecular density as for $^{13}CO_2$, since our data analysis assumes that the two molecular densities are the same. At this 2.04% higher pressure of 66.65 bar, the $^{12}CO_2$ sample has a 1.16% higher molecular density (0.009 952(2) Å$^{-3}$) as compared to that of the $^{12}CO_2$ sample at 65.32 bar (0.009 838(2) Å$^{-3}$) shown in figure 8 (molecular densities from (Span and Wagner 1996)). We therefore need to explain why $^{13}CO_2$ would have a 1.16% higher molecular density than $^{12}CO_2$ at a given pressure in our experiments.

For a system of atoms interacting via a given set of potentials, classical statistical mechanics predicts that the structure, as measured by diffraction, is independent of the masses of the atoms (e.g. Egelstaff 1992 sections 5.3 and 8.4). Any measured changes in structure (including atomic or molecular number density) resulting from isotopic substitution are therefore called 'quantum effects', which can be conveniently observed via x-ray diffraction since the scattering lengths are independent of isotopic mass. For

instance, a 1.6% change in the measured x-ray diffraction intensity has been observed for $D_2O$ versus $H_2O$ (Tomberli *et al* 2000), resulting from a 0.5% molecular density difference (Badyal *et al* 2002) at ambient conditions.

A general conclusion resulting from these QM-effect experiments is that the heavier isotope sample tends to have a more ordered structure, since its QM zero-point motion amplitude is smaller. Recall that at room temperature bending and stretching modes of molecules such as $CO_2$ can be close to the QM ground state. One would therefore expect the $^{13}CO_2$ sample to have a slightly higher molecular number density at a given $T$ and $P$, which goes in the right direction to explain our diffraction data. However, a molecular density difference of 1.16% is about a factor of two larger than that observed for $D_2O$ versus $H_2O$, and furthermore, the $^{13}C/^{12}C$ mass ratio is much smaller than for D/H.

Our $CO_2$ experiments were however performed relatively close to the critical point of $^{nat}CO_2$ ($T_c = 304.12$ K, $P_c = 73.77$ bar) at a molecular density of about 1.5 times that of $\rho_c$. Our samples were therefore quite compressible, which should render them more susceptible to QM effects. To get an estimate of this factor, consider the difference between the critical points of $H_2O$ ($T_c = 647.096$ K, $P_c = 220.64$ bar) and $D_2O$ ($T_c = 643.847$ K, $P_c = 216.71$ bar). The molecular density of $H_2O$ at $D_2O$'s critical point is 50% higher than for $H_2O$ at its own critical point (Span and Wagner 1996).

Furthermore, at a temperature 2% below $H_2O$'s $T_c$ and close to the gas/liquid equilibrium line, analogous to the situation for our $CO_2$ experiments, the molecular density difference between $H_2O$ and $D_2O$ is still 6.6%. Now, the molecular mass ratio for $D_2O/H_2O$ is $20/18 = 1.111$ (i.e. 11.1%), whereas for $^{13}CO_2/^{12}CO_2$ it is only $45/44 = 1.0227$ (i.e. 2.27%). Scaling by this difference in average molecular mass ratios, one could expect something like a $6.6\% \times (2.27/11.1) = 1.35\%$ difference in molecular density between $^{13}CO_2$ and $^{12}CO_2$ due to QM effects at the $(T, P)$ of our diffraction experiments, which corresponds to slightly more than we have observed. As mentioned in the introduction, however, the carbon atom's central position in the $CO_2$ molecule would tend to reduce QM effects from $^{13}C/^{12}C$ substitution, since its mass is not a factor for symmetric vibration modes at least, whereas the H and D isotopes appear at the extremities of the water molecule. On the other hand, we could expect some enhancement of QM effects in our $CO_2$ diffraction results, since the experiments were performed at an absolute temperature about half that of the analogous $H_2O/D_2O$ temperature.

In any case, a higher molecular density for $^{13}CO_2$ versus $^{12}CO_2$ remains speculative in the absence of direct measurements to this purpose. We can however propose that the value of $b_{\mathrm{incoh,13C}} = 0.42 \pm 0.24$ fm obtained from our $CS_2$ diffraction data is likely to be consistent with our $CO_2$ diffraction data once account is made of QM effects arising from the isotopic mass difference. Note that the $CS_2$ molecular density would be much less affected by QM effects than $CO_2$ because of a larger molecular mass and a much greater distance from criticality.

### *3.7. The spin-dependent scattering lengths $b_+$, $b_-$ and the sign of $b_{incoh}$*

The incoherent scattering of an isotope comes from its possible nuclear spin $I$ that may be projected either parallel or anti-parallel onto the incident neutron's spin. For $I \neq 0$, this leads to two spin-dependent scattering lengths $b_+$ (up) and $b_-$ (down). In our case of a non-polarized scattering system, the isotope's coherent and incoherent scattering lengths can be expressed as

$$b_{\mathrm{coh}} = \overline{b} = \frac{I+1}{2I+1} b_+ + \frac{I}{2I+1} b_- \tag{3.7}$$

and

$$b^2_{\mathrm{incoh}} = \frac{I(I+1)}{(2I+1)^2} (b_+ - b_-)^2 \tag{3.8}$$

giving

$$b_{\mathrm{incoh}} = \frac{\sqrt{I(I+1)}}{(2I+1)} (b_+ - b_-) \tag{3.9}$$

upon applying the standard sign convention for $b_{\mathrm{incoh}}$. The zero spin of the isotope $^{12}C$ results in $b_{\mathrm{incoh,12C}} = 0$, whereas $^{13}C$ has $I = 1/2$ and leads to the following expressions:

$$b_{\mathrm{coh,13C}} = \overline{b}_{\mathrm{13C}} = \tfrac{3}{4} b_{\mathrm{+13C}} + \tfrac{1}{4} b_{\mathrm{-13C}} \tag{3.10}$$

and

$$b_{\mathrm{incoh,13C}} = \frac{\sqrt{3}}{4} (b_{\mathrm{+13C}} - b_{\mathrm{-13C}}) \tag{3.11}$$

which are easily solved for the spin-dependent scattering lengths,

$$b_{\mathrm{+13C}} = b_{\mathrm{coh,13C}} + \frac{1}{\sqrt{3}} b_{\mathrm{incoh,13C}} \tag{3.12}$$

and

$$b_{\mathrm{-13C}} = b_{\mathrm{coh,13C}} - \frac{3}{\sqrt{3}} b_{\mathrm{incoh,13C}}. \tag{3.13}$$

There appears to be good agreement in the literature that the sign of $^{13}C$'s incoherent scattering length is negative, implying $b_{\mathrm{+13C}} < b_{\mathrm{-13C}}$. The currently accepted value of $b_{\mathrm{incoh,13C}} = -0.52(9)$ fm from Glättli *et al* (1979) is consistent with the theoretical result of $-0.4$ fm by Normand (1977) and has the same sign as the value of $-0.26$ fm deduced from the work of Aleksejevs *et al* (1998).

On adopting this negative sign, the final value from our diffraction data becomes

$$b_{\mathrm{incoh,13C}} = -0.42 \pm 0.24 \text{ fm},$$

and thus $b_{\mathrm{+13C}} - b_{\mathrm{-13C}} = -0.97(55)$ fm from equation (3.11). Using our result for $b_{\mathrm{coh,13C}} = 6.542(3)$ fm and equations (3.12) and (3.13), we can then derive spin-dependent scattering lengths of

$$b_{\mathrm{+13C}} = 6.30(14) \text{ fm} \qquad \text{and} \qquad b_{\mathrm{-13C}} = 7.27(42) \text{ fm},$$

which are not very consistent with the values of $b_{\mathrm{+13C}} = 5.6(5)$ fm and $b_{\mathrm{-13C}} = 6.2(5)$ fm as tabulated by Rauch and Waschkowski (2002) and derived from the data-fitting calculations of Aleksejevs *et al* (1998). By contrast, the result

of Glättli *et al* (1979) for $b_{+13C} - b_{-13C} = -1.2(2)$ fm, when combined with our value for $b_{coh,13C}$, leads to $b_{+13C} = 6.24(5)$ fm and $b_{-13C} = 7.44(16)$ fm, which are consistent with our values for the spin-dependent scattering lengths, as expected.

We can also use our value for $b_{incoh,13C} = -0.42(24)$ fm to calculate the expected incoherent neutron scattering cross-section of natural carbon: $\sigma_{incoh,natC} = 4\pi b^2_{incoh,natC}$, or equivalently its thereby defined incoherent scattering length $b_{incoh,natC}$. Using our results for $b_{coh,13C} = 6.542(3)$ fm and $b_{coh,12C} = 6.6496(13)$ fm, and the isotopic concentrations of 1.11% $^{13}$C and 98.89% $^{12}$C, we easily calculate an isotopic variation contribution of only $4\pi \mathrm{var}(b_{coh}) = 0.016$ mb, as compared to $^{13}$C's spin contribution of $4\pi b^2_{incoh,13C} \times 0.0111 = 0.24(28)$ mb, leading to a total $\sigma_{incoh,natC} = 0.26(28)$ mb. This value is consistent with the standard tabulated value of 1(4) mb (Sears 1992). In terms of incoherent scattering length, we obtain $b_{incoh,natC} = 0.045(24)$ fm, which agrees with the standard value of 0.09(18) fm listed in table 1.

## 4. Summary and conclusions

Motivated by the need for accurate values of carbon's neutron scattering lengths, especially as regards neutron diffraction with isotopic substitution (NDIS) studies, we undertook neutron interferometry and neutron diffraction experiments involving $^{13}$C-substituted liquid $CS_2$ and liquid $CO_2$ samples. Our interferometry result of $b_{coh,13C} = 6.542(3)$ fm for the bound coherent scattering length of $^{13}$C differs, beyond estimated experimental uncertainties, from the currently accepted value of 6.19(9) fm measured by Koester *et al* (1979). Our result is however entirely consistent with the value of 6.56(3) fm obtained by Young *et al* (1997) via structural refinement of the single-crystal neutron diffraction intensity for a partially $^{13}$C-substituted organic molecule.

Having paid particular attention to the data analysis and to the control of possible experimental errors, we propose our result of $b_{coh,13C} = 6.542(3)$ fm as a new standard value for the bound coherent neutron scattering length of the $^{13}$C isotope.

Concerning our neutron diffraction result of $b_{incoh,13C} = -0.42(24)$ fm for the bound incoherent scattering length of $^{13}$C, its accuracy is limited by the chemical purity of the $^{13}CS_2$ sample, and by knowledge of the molecular density of $^{13}CO_2$ close to its critical point. We note simply that our value for $b_{incoh,13C}$ is completely consistent with both the standard tabulated value of $-0.52(9)$ fm obtained by Glättli *et al* (1979), and with the theoretical result of $-0.4$ fm by Normand (1977).

The results presented here lead to a bound coherent scattering length contrast between $^{13}$C and $^{nat}$C of only 0.106(3) fm, more than a factor of four smaller than given by standard tables, but consistent with previously attempted NDIS studies, and sufficient to permit a determination of partial structure factors when combined with x-ray diffraction data Neuefeind *et al* (2008).

## Acknowledgments

We thank Pierre Palleau (ILL) for his valuable assistance in preparing the neutron scattering experiments, as well as Isabelle Grillo and Jürgen Klepp for their help with the UV–vis spectrophotometer absorption measurements. We also appreciate informative discussions with Adrian Barnes and Phil Salmon, as well as helpful advice from Phil Mason concerning the $CS_2$ samples. The mass spectrometry measurements on $CO_2$ were performed by R Ilgner.

The Spallation Neutron Source (SNS) is managed by UT-Battelle, LLC, under contract DEAC05-00OR22725 for the US Department of Energy. Contributions of JMS to this research were conducted at the Center for Nanophase Materials Sciences, which is sponsored at Oak Ridge National Laboratory by the Division of Scientific User Facilities, US Department of Energy.

## References

Aleksejevs A, Barkanova S, Tambergs J, Krasta T, Waschkowski W and Knopf K 1998 *Z. Naturf.* A **53** 855–62
Badyal Y S, Price D L, Saboungi M-L, Haeffner D R and Shastri S D 2002 *J. Chem. Phys.* **116** 10833
Egelstaff P A 1992 *An Introduction to the Liquid State* 2nd edn (Oxford: Oxford University Press)
Fischer H E, Barnes A C and Salmon P S 2006 *Rep. Prog. Phys.* **69** 233–99
Fischer H E, Cuello G J, Palleau P, Feltin D, Barnes A C, Badyal Y S and Simonson J M 2002 *Appl. Phys.* A **74** S160–2
Freund A K, Kischko U, Bonse U and Wroblewski T 1985 *Nucl. Instrum. Methods* A **234** 495–7
Garcia Baonza V, Nuñez Delgado J and Caceres Alonso M 1989 *J. Chem. Thermodyn.* **21** 231–6
Glättli H, Bacchella G L, Fourmond M, Malinovski A, Meriel P, Pinot M, Robeau R and Abragam A 1979 *J. Physique* **40** 629–34
Houk T L 1971 *Phys. Rev.* C **3** 1886
Howe M A, McGreevy R L and Zetterström P 1998 CORRECT: a correction program for neutron diffraction data *Studsvik Neutron Research Laboratory Report* March 1998 (unpublished)
Kameda Y, Sasaki M, Yaegashi M, Tsuji K, Oomori S, Hino S and Usuki T 2004 *J. Sol. Chem.* **33** 733–45
Koehler W C and Wollan E O 1952 *Phys. Rev.* **85** 491
Koester L, Knopf K and Waschkowski W 1979 *Z. Phys.* A **292** 95
Koester L and Nistier W 1975 *Z. Phys.* A **272** 189
Koester L, Rauch H and Seymann E 1991 *At. Data Nucl. Data Tables* **49** 65
Kroupa G, Bruckner G, Bolik O, Zawisky M, Hainbuchner M, Badurek G, Buchelt R J, Schricker A and Rauch H 2000 *Nucl. Instrum. Methods* A **440** 604–8
Mason P 2005 private communication
Mopsik F I 1969 *J. Chem. Phys.* **50** 2559–69
Mughabghab S F, Divadeenam M and Holden N E (ed) 1981 *Neutron Cross Sections* vol 1, part A (New York: Academic)
Neuefeind J, Fischer H E and Schröer W 2000 *J. Phys.: Condens. Matter* **12** 8765
Neuefeind J, Fischer H E, Simonson J M, Idrissi N, Schöps A and Honkimäki V 2008 in preparation
Normand J M 1977 *Nucl. Phys.* A **291** 126
Placzek G 1952 *Phys. Rev.* **86** 377
Rauch H and Waschkowski W 2002 *Neutron Data Booklet* ed A J Dianoux and G Lander (Grenoble: Institut Laue-Langevin) chapter 1.1
Rauch H and Werner S A 2000 *Neutron Interferometry: Lessons in Experimental Quantum Mechanics* (Oxford: Clarendon)
Sears V F 1992 *Neutron News* **3** 26–37 on-line at http://www.ncnr.nist.gov/resources/n-lengths/
Span R and Wagner W 1996 *J. Phys. Chem. Ref. Data* **25** 1509 with on-line version available at http://webbook.nist.gov/chemistry/fluid/

Tomberli B, Benmore C J, Egelstaff P A, Neuefeind J and Honkimäki V 2000 *J. Phys.: Condens. Matter* **12** 2597–612
Turner J, Finney J L and Soper A K 1991 *Z. Naturf.* A **46** 73
Weill B 2007 private communication (Hellma-France)
Yarnell J L, Katz M J, Wenzel R G and Koenig S H 1973 *Phys. Rev.* A **7** 2130
Young D M, Schultz A J, Kini A M and Williams J M 1997 *Acta Crystallogr.* C **53** 961